Research article

Age-dependent increase in Thy-1 protein in the rat supraoptic nucleus

Jason M. Askvig [*], Talia S. Dalzell, Nadia Toumeh, Phillip T. Kuball, Sara T. Whiteman, Erik W. Bye, Marissa J. Andersen, Michael G. McCarthy, Riley E. Irmen, Sydney H. Bexell, Molly M. Benolken, Brooke L. Maruska, Shelby E. Nordmann

Department of Biology, Concordia College, Moorhead, MN, 56562, USA

A B S T R A C T

Mature mammalian CNS neurons often do not recover successfully following injury. To this point, unilateral lesion of the hypothalamo-neurohypophysial tract results in collateral sprouting from uninjured axons of the supraoptic nucleus (SON) in 35-day-old but not in 125-day-old rats. Thus, it appears that there are age-related changes within the SON that preclude the older rat from recovering following axotomy. We hypothesize that the intrinsic capacity for axon reorganization may depend, in part, on age-related alterations in cell adhesion molecules that allow normal astrocyte-neuron interactions in the SON. In support of our hypothesis, numerous reports have shown that Thy-1 is increased in neurons at the cessation of axon outgrowth. Therefore, we compared protein levels of Thy-1 and the Thy-1 interacting integrin subunits, alpha-v (α_v), beta-3 (β_3), and beta-5 (β_5), in 35- and 125-day-old SON using western blot analysis. Our results demonstrated that there was significantly more Thy-1 protein in the 125-day-old SON compared to 35-day-old SON, but no change in the protein levels of the integrin subunits. Furthermore, we localized Thy-1-, α_v integrin-, β_3 integrin-, and β_5 integrin-immunoreactivity to both neurons and astrocytes in the SON. Altogether, our results suggest that the observed increase in Thy-1 protein levels in the SON with age may contribute to an environment that prevents collateral axonal sprouting in the SON of the 125-day-old rat.

1. Introduction

It is well understood that the aging brain has a decreased capacity to recover following injury. This may be due in part to localized changes to the neuronal and glial intrinsic and extrinsic environment as the animal ages. The magnocellular neurosecretory system, which contains oxytocin- and vasopressin-producing magnocellular neurons with their somata located in the supraoptic nucleus (SON) and their axons that project via the infundibulum to terminate in the neural lobe (NL; posterior pituitary), has been extensively studied following axotomy. Numerous reports have shown that injury to the axons of the magnocellular neuron results in post-injury regenerative growth (Moll, 1957; Moll and de Wied, 1962; Adams et al., 1964; Kiernan, 1970, 1971; Raisman, 1973; Polenov et al., 1974; Kawamoto and Kawashima, 1985; Watt and Paden, 1991; Watt et al., 1999). To this point, previous reports demonstrated that unilateral lesion of the hypothalamo-neurohypophysial tract, which severs the axons in the ipsilateral SON while sparing the contralateral SON axons, results in the loss of 42% of the axons in the NL at one-week post-lesion, followed by a collateral sprouting response to return the axon numbers to control levels by four-week post-lesion in 35-day-old (35d) rats (Watt and Paden, 1991; Watt et al., 1999). Conversely, unilateral lesion in 125-day-old (125d) rat does not induce a collateral axonal sprouting response (Askvig and Watt, 2019), indicating that a loss of axonal plasticity in the rat SON occurs between 35d and 125d. What promotes the post-injury collateral sprouting response in the 35d rat and what changes occur in the SON between 35d and 125d rats that precludes the sprouting response following injury in the 125d rat has yet to be determined.

Our central hypothesis is that the post-injury sprouting response following unilateral lesion is promoted by ciliary neurotrophic factor (CNTF), which is only found in astrocytes in the SON (Watt et al., 2006). In support of this hypothesis, our lab, and others, have shown that CNTF promotes axonal sprouting (Askvig and Watt, 2015) and neuron survival (Vutskits et al., 1998; Rusnak et al., 2002, 2003; Askvig et al., 2013; Askvig and Watt, 2015) following axotomy in hypothalamic organotypic cultures containing the SON. Moreover, CNTF protein levels are elevated during the sprouting response in the 35d rat SON (Watt et al., 2006; Askvig et al., 2012), and the CNTF specific receptor, CNTF receptor alpha

---

(CNTFRα), is decreased in the absence of injury in the 125d rat SON (Askvig and Watt, 2019). Collectively, these data suggest that CNTF may be involved in the axonal sprouting from uninjured neurons following unilateral lesion. Although, if CNTF does promote the collateral sprouting response in the SON it has to act indirectly via astrocytes, which are the only cell in the SON that contains all three (CNTFRα, LIFRß, and gp130) of the CNTF receptor components (Askvig et al., 2012). Thus, we believe understanding the cellular interactions between astrocytes and neurons in the SON will be paramount to understanding the possible post-injury role that CNTF plays in the SON.

Previous reports have demonstrated that CNTF expression is down-regulated by cell adhesion molecule interactions (CAMs), specifically, interactions between neuronal Thy-1 and astrocytic $\alpha_V\beta_5$ integrin (Kang et al., 2012; Keasey et al., 2013). Within the nervous system, the functions of CAMs are diverse but are primarily focused with general cellular adhesion, myelin formation, synapse formation, neurite bundling, and gap junction formation (Shapiro et al., 2007). Numerous reports demonstrate that CAMs are necessary for neurite outgrowth and axon guidance during development (Georges-Labouesse et al., 1998; Gupton and Gertler, 2010; Harper et al., 2010), in addition to promoting neuron survival and axonal sprouting functions following axotomy (Gardiner et al., 2005, 2007; Vogelezang et al., 2007). More specifically, integrin proteins have been linked to the inhibition of axon outgrowth, specifically due to their interaction with Thy-1 (Herrera-Molina et al., 2012). Thy-1 (thymocyte antigen 1, CD90) is a GPI-anchored glycoprotein found on the extracellular surface of neurons and has been shown to inhibit axon outgrowth by interacting with integrins on astrocytes (Tiveron et al., 1992; Leyton et al., 2001; Avalos et al., 2002, 2004, 2009). Integrins function as heterodimers of transmembrane polypeptides, alpha (α) and beta (ß) chains, and $\alpha_V\beta_3$ (Leyton et al., 2001; Hermosilla et al., 2008; Avalos et al., 2009) and $\alpha_V\beta_5$ (Zhou et al., 2010; Keasey et al., 2013) have been shown to be the astrocytic receptors for neuronal Thy-1. Thus, these reports suggest that neuronal Thy-1 and astrocytic integrins may be involved in preventing or repressing axonal outgrowth. While Thy-1 is present in axons of magnocellular neurons at the site of the axon terminals in the NL (Miyata et al., 2001), to date, little is known about Thy-1 or integrin protein localization in the SON. Therefore, we sought to characterize the cellular localization of Thy-1, α_V integrin, β_3 integrin, and β_5 integrin in the SON and determine if the protein levels of these CAMs change with age in the SON and NL. We believe these experiments will help clarify the age-dependent changes following axotomy to the neurons in the SON as well as the role that CNTF may play in promoting the post-injury collateral sprouting response in the NL.

2. Materials and methods

2.1. Animals

We purchased male Sprague-Dawley rats from Envigo (Minneapolis, MN) and they were housed in the vivarium in the Integrated Science Center on the campus of Concordia College under a 12L:12D light cycle with ad libitum access to lab chow and tap water. Animal care protocols utilized in these studies complied with all appropriate federal and state laws, as well as with NIH guide for the care and use of laboratory animals, with approval from the Concordia College Institutional Animal Care and Use Committee (#AUP_BIO_2018.03). Rats used in this study were received between 30-35 or 120–125 days of age and were allowed to adapt to the colony room for several days before sacrifice between either 35–40 days of age (75–100 g) or 125–130 days of age (450–550 g).

2.2. Gel electrophoresis and western blot

Experimental procedures were conducted as previously stated (Askvig et al., 2012, 2013; Askvig and Watt, 2019). Once the rats were approximately 35- or 125-days old, they were anesthetized with sodium pentobarbital (35 mg/kg, i.p.; Sigma; St. Louis, MO) (Deacon and Rawlins, 1996), decapitated,

and their brains were removed intact. SON and NL samples were carefully dissected under a dissecting microscope and pooled from three rats in a solution of radioimmuno-precipitation assay buffer containing 1% protease inhibitor (Sigma) and 1% phosphatase inhibitor (Sigma). The tissue samples were then sonicated and centrifuged at 4 °C. We used the bicinchoninic acid colorimetric detection assay (Pierce BCA Protein Assay; Pierce) to determine total protein content in the SON and NL samples, and supernatant from each sample was stored at -80 °C until needed.

Using a 12% SDS-PAGE gel (Precise Protein Gels; Pierce), each lane was loaded with 25 µg of protein from the SON or NL, and proteins were separated at 90 V for approximately 1.25 h and then electrophoretically transferred to a PVDF membrane (0.2 µm; Bio-Rad, Hercules, CA) at 70 V for 2 h. After blocking non-specific binding sites with the appropriate blocking buffer listed according to the antibody data sheet (5% bovine serum albumin or 5% milk in phosphate-buffered saline (PBS) plus 0.1% Tween-20), we incubated the membrane overnight at 4 °C in mouse anti-Thy-1 (1:1000; #MAB1406, Millipore; Burlington, MA). The membranes were then washed repeatedly for 1 h in PBS-Tween and incubated for 2 h in the species-appropriate HRP-conjugated secondary antibody (1:50,000; Santa Cruz Biotechnology; Santa Cruz, CA). The bands were subsequently visualized following 2 h of PBS washes using the West Femto chemiluminescent detection kit (Pierce) with chemiluminescence film (Amersham Hyperfilm ECL; GE Healthcare; VWR; West Grove, PA) developed in a darkroom using Kodak film development chemicals (Sigma). Afterward, bound antibodies were removed with stripping buffer (pH 2.2; 15g glycine; Sigma, 1g SDS; Bio-Rad, 10 ml Tween-20; Bio-Rad in 1 L ultrapure water). The previously listed steps were repeated to sequentially reprobe the membrane for the following antibodies; rabbit anti-α_V integrin (1:1000; #4711, Cell Signaling Technology, Inc., Danvers, MA), rabbit anti-β_3 integrin (1:2000; #13166, Cell Signaling), rabbit anti-β_5 integrin (1:1000; #3629, Cell Signaling), and mouse anti-ß-actin (1:50,000; #A2228, Sigma).

Densitometric analysis of immunoblot signals was performed using Image J (NIH). Digitized western blot films were opened in Image J, bands of interest were outlined with a rectangle, and the areal density of the band was calculated by histogram analysis. The density of all bands was normalized to ß-actin band density to obtain ratios. The analysis was repeated on three separate samples per group resulting in mean ratio values for each group that was used for statistical analysis as described below.

2.3. Dual-label fluorescent immunocytochemistry

Experimental procedures were conducted as previously stated (Askvig et al., 2012, 2013). Rats were anesthetized with sodium pentobarbital (50 mg/kg, i.p.) and transcardially perfused with approximately 50 mL of 0.9% saline followed by approximately 500 mL of periodate-lysine-paraformaldehyde fixative (PLP; 3.2% para-formaldehyde, 2.2% lysine, 0.33% sodium-(meta) periodate; Sigma) that was prepared immediately before use (McLean and Nakane, 1974). Brains were removed, trimmed to contain the SON, and post-fixed in PLP overnight before cryoprotection in 25% sucrose in PBS. Cryosections (16 µm) were obtained using a cryostat (Microm HM550; Fisher Scientific) and mounted on gelatin-coated slides and stored at -20 °C until use.

Cryosections were washed with PBS containing 0.3% Triton X-100 (PBS-T; Sigma) in 5 × 10 min intervals before and after all incubations. Non-specific staining was alleviated by treatment with blocking buffer (4% of the appropriate normal serum (Vector, Burlingame, CA) in PBS-T) for 1 h at room temperature before an overnight incubation at 4 °C in mouse anti-Thy-1 (1:50; #MAB1406, Millipore), rabbit anti-α_V integrin (1:25; #60896, Cell Signaling), rabbit anti-β_3 integrin (1:25; #13166, Cell Signaling), or rabbit anti-β_5 integrin (1:50; #3629, Cell Signaling). Sections were then incubated in the species-appropriate biotinylated IgG secondary antibody (1:500; Vector) for 1 h followed by either the astrocyte-specific antibody, mouse anti-GFAP (1:1000; #G-3893, Sigma), or a SON neuron-specific antibody, guinea pig anti-oxytocin (1:1000; #T-5021, Peninsula Laboratories, San Carlos, CA) or guinea pig anti-

vasopressin (1:1000; #T-5048, Peninsula Laboratories). The antibodies were fluorescently labeled using a cocktail of Alexa streptavidin 488 or 594 (1:1000; Molecular Probes, Eugene, OR) with species-specific secondary IgG conjugated to either Alexa Fluor 488 or Alexa Fluor 594 (1:200; Molecular Probes) and cryosections were coverslipped using Vectashield mounting medium (Vector).

Images of the SON were acquired using 20x, 60x oil-immersion, or 100x oil-immersion objectives on an Olympus BX-51 fluorescent microscope with mounted DP-71 color camera and dedicated software. Colocalization of Thy-1 and the integrin subunits with neuronal or astrocytic markers were quantified with ImageJ software using the colocalization colormap plugin to calculate the Correlation Index (Icorr) (Jaskolski et al., 2005), which indicates the fraction of positively correlated pixels in the image. For each antibody of interest, we performed quantitative analysis from a minimum of three rats and used at least three cryosections sampled throughout the entire rostral-caudal SON. To ensure that the same cells were not analyzed twice, a minimum of five sections (80 μm) were skipped before the next cryosection was immunocytochemically processed. The DP-71 camera software was used to adjust the brightness and contrast on an entire image while avoiding the misrepresentation of any information present in the original image while treating every pixel in each image the same.

As a control for the dual-label fluorescence immunocytochemistry, incubations with the antibodies for the proteins of interest (Thy-1 and integrin subunits) on separate cryosections were followed by incubation with the species-specific fluorescent-conjugated secondary antibodies for the cell-specific markers (anti-GFAP, -OT, and -VP). Similarly, tissue that was incubated with the anti-GFAP, -OT, or -VP antibodies was exposed to the fluorescent-conjugated secondary antibodies for Thy-1 or the integrin subunits. These controls demonstrated an absence of fluorescent immunoreactivity in the rat SON, indicating that the fluorescent-conjugated secondary antibodies were specific for their appropriate primary antibody, and there was no observable cross-reactivity between the secondary antibodies (data not shown).

2.4. Statistical analysis

Quantitative data was tested for distribution normality using the Kolmogorov-Smirnov test for normality (GraphPad Prism, version 6.0; San Diego, California). Individual group comparisons were performed using Student's *t* test with *p < 0.05* considered as statistically significant. Results presented herein are expressed as the group means ± SD.

3. Results

3.1. Thy-1 protein increases with age in the SON

Western blot analysis demonstrated a statistically significant increase of 801% in Thy-1 protein levels in the 125d SON compared to the 35d SON (*p=0.0245*; Figure 1a). However, we found no significant change in α_V integrin protein levels (*p=0.7441*; Figure 1b), β_3 integrin protein levels (*p=0.9452*; Figure 1c), or β_5 integrin protein levels (*p=0.6292*; Figure 1d) in the 125d SON compared to the 35d SON. Protein analysis in the NL demonstrated no significant change in Thy-1 protein levels (*p=0.6837*; Figure 2a), α_V integrin protein levels (*p=0.8905*; Figure 2b), β_3 integrin protein levels (*p=0.7624*; Figure 2c), or β_5 integrin protein levels (*p=0.2731*; Figure 2d) in the 125d NL compared to the 35d NL. Together, these data indicate that as the rat ages, there is more Thy-1 protein in the SON but no change in the integrin subunits in the SON or NL between 35d and 125d.

3.2. Thy-1-, α_V integrin-, β_3 integrin-, and β_5 integrin-immunoreactivity is localized to magnocellular neurons and astrocytes in the SON

We performed quantitative dual fluorescent analysis of Thy-1, α_V integrin, β_3 integrin, and β_5 integrin to identify the cells that express

these CAMs within the SON. We observed robust immunoreactivity for Thy-1 in neuronal somata distributed throughout the SON and dual-label immunocytochemistry confirmed the presence of Thy-1-immunoreactivity associated with both oxytocinergic (Figure 3a-c) and vasopressinergic (not shown) magnocellular neurons. While the Thy-1 immunoreactive profiles were consistently found in the magnocellular neurons of the SON, we only sporadically observed Thy-1 colocalization within GFAP-immunoreactive astrocytes in the SON (Figure 3d-f). Using the colocalization colormap plugin for ImageJ, we quantified the levels of Thy-1-immunoreactivity and our results demonstrated significantly more
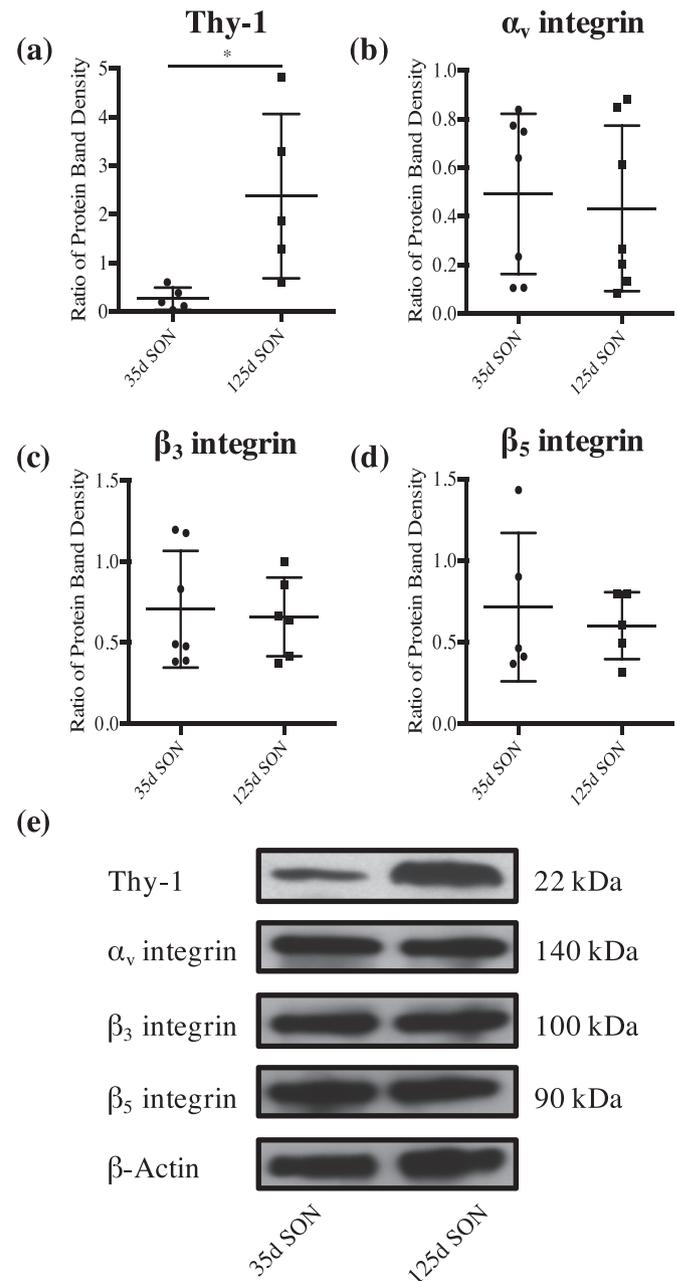
Figure 1. More Thy-1 protein present in the 125d SON. Western blot analysis revealed a significant increase of 801% in Thy-1 protein levels in the 125d SON compared to 35d SON (a; *p=0.0245*). Additionally, our results revealed no change in protein levels of α_V integrin (b; *p=0.74*), β_3 integrin (c; *p=0.95*), or β_5 integrin (d; *p=0.63*) in the 125d SON compared to 35d SON. Representative protein bands with their molecular weights are presented in (e). Each shape on the graph indicates an individual data point with the lines representing the mean and SD. Each data point represents isolated SON pooled from three rats and analysis was repeated on three separate samples per group.

(a) Thy-1

(b) α_v integrin

(c) β_3 integrin
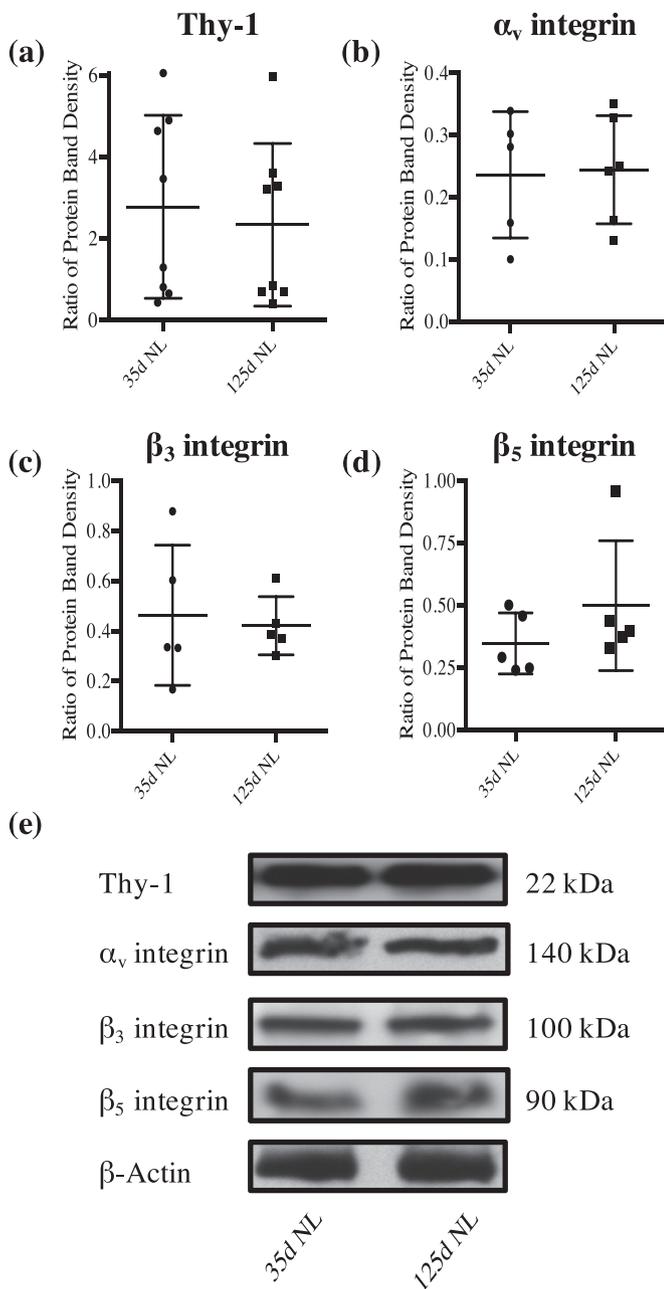
(d) β_5 integrin

Figure 2. No change in Thy-1 or integrin subunit protein levels between 35d and 125d in the NL. Western blot analysis revealed no change in Thy-1 protein levels (a; $p=0.68$), α_V integrin (b; $p=0.89$), β_3 integrin (c; $p=0.76$), or ß$_5$ integrin (d; $p=0.27$) in the 125d NL compared to 35d NL. Representative protein bands with their molecular weights are presented in (e). Each shape on the graph indicates an individual data point with the lines representing the mean and SD. Each data point represents isolated SON pooled from three rats and analysis was repeated on three separate samples per group.

Thy-1-immunoreactivity was present in neurons compared to astrocytes ($p=0.001$; Figure 3g).

Dual fluorescent analysis of the integrin subunits demonstrated weak, but consistent cytosolic immunoreactivity for α_V integrin in neuronal somata with more robust α_V integrin-immunoreactivity in the ventral glial limitans (VGL), which is the primary location for the GFAP-immunoreactive astrocytes in the SON. Quantitative analysis demonstrated consistent levels of α_V integrin-immunoreactive profiles in both neurons (Figure 4a-c) and astrocytes (Figure 4d-f) in the SON ($p=0.0762$; Figure 4g). Similarly, we observed robust, cytosolic immunoreactivity for

ß$_3$ integrin throughout the entire SON and found ß$_3$ integrin-immunoreactive profiles co-localized with vasopressinergic magnocellular neurons (data not shown) and oxytocinergic magnocellular neurons (Figure 5a-c). Even though ß$_3$ integrin-immunoreactivity was weak in the VGL of the SON, we did observe consistent colocalization with astrocytes in the SON (Figure 5d-f) and quantification demonstrated no difference in ß$_3$ integrin colocalization between neurons or astrocytes ($p=0.119$; Figure 5g). We observed a consistent band of ß$_5$ integrin-immunoreactivity in the VGL of the SON with robust ß$_5$ integrin-immunoreactivity throughout the rest of the SON. Our results demonstrated colocalization of ß$_5$ integrin protein in vasopressinergic magnocellular neurons (Figure 6a-c), oxytocinergic magnocellular neurons (data not shown), and GFAP-immunoreactive astrocytes of the SON (Figure 6d-f). Quantification demonstrated no difference in the ß$_5$ integrin colocalization between neurons or astrocytes ($p=0.4018$; Figure 6g). Altogether, the results of our dual fluorescent analysis indicate that Thy-1, α_V integrin, ß$_3$ integrin, and ß$_5$ integrin are co-localized to neurons and astrocytes of the SON.

4. Discussion

Multiple reports establish that the brain is less plastic with age, and thus, the ability to functionally recover following injury is diminished in older animals (Shetty and Turner, 1998; Buga et al., 2008a, 2008b; Luo et al., 2010; Jaerve et al., 2011). It remains to be determined what facilitates the age-dependent decline in plasticity in the CNS, but several hypotheses exist, many of which are focused on age-dependent changes in anti-sprouting or pro-sprouting molecules. We have demonstrated that the same injury induces collateral sprouting from uninjured axons in 35d rat, but not in the 125d rat (Watt and Paden, 1991; Watt et al., 1999; Askvig and Watt, 2019). Our and others' research supports our hypothesis that CNTF promotes the axonal sprouting in the SON of 35d rats (Watt et al., 2006, 2009; Askvig et al., 2012, 2013) and our interest in Thy-1 and integrins arises from the evidence that in the rat SON the astrocytes are the only cell capable of directly responding to CNTF due to astrocytic localization of the tripartite CNTF receptor complex (Askvig et al., 2012). Moreover, CNTF is inhibited via Thy-1-α_Vß$_5$ integrin interaction and the absence of neuron-astrocyte interaction increases CNTF *in vitro* (Kang et al., 2012; Keasey et al., 2013). Thus, understanding the presence of CAMs in the SON may help determine how CNTF can induce astrocytes to communicate with neurons to promote postinjury neuroregenerative responses.

During early development, neuronal expression of Thy-1 is low, but Thy-1 increases in neurons with age (Xue et al., 1990; Barlow and Huntley, 2000). Additionally, Thy-1 is not expressed on axons until axonal growth is complete (Morris and Grosveld, 1989; Xue et al., 1991), and increased Thy-1 expression with age has been shown to block neuronal repair in astrocyte-rich regions of the mature brain (Tiveron et al., 1992). Since Thy-1 gradually increases with age in the brain, the increase in Thy-1 protein in the SON that we observed is not surprising. However, it remains to be determined if increased Thy-1 prevents axonal outgrowth or if the cessation of axonal outgrowth increases Thy-1. It should be noted that there are reports that Thy-1 promotes axon outgrowth (Doherty et al., 1993; Dreyer et al., 1995), though, the majority of the literature suggests that Thy-1 functions as an axon outgrowth inhibitor, possibly by clustering Thy-1 and stabilizing the surface-membrane complexes formed by Thy-1 with the underlying cytoskeleton (Herrera-Molina et al., 2012, 2013). Considering the numerous reports indicating the role of Thy-1 in preventing axon growth and our previous reports demonstrating the absence of axonal sprouting following injury in the 125d rat, our data demonstrating increased Thy-1 in the 125d rat SON suggests that Thy-1 may be involved in prohibiting the sprouting response in the 125d rat that normally occurs following injury in the 35d rat SON, when there is significantly less Thy-1 present.

Cellular localization of Thy-1 and integrin subunits in the SON had not been reported, although Thy-1 was previously localized to axons of
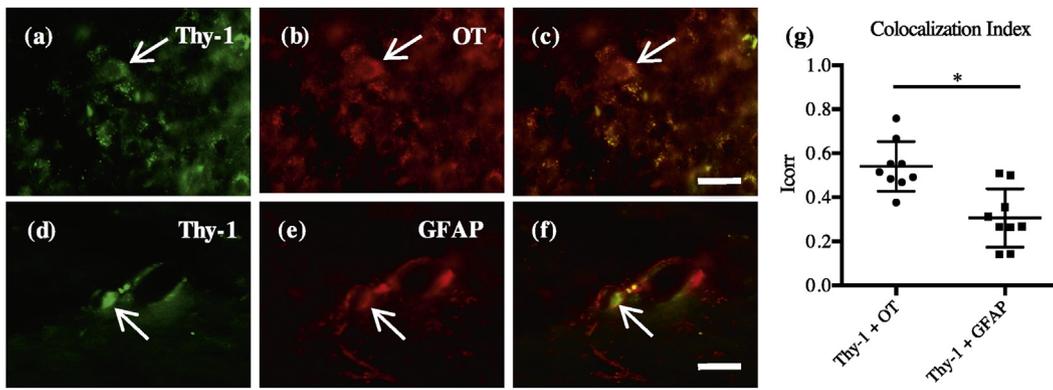
Figure 3. Thy-1-immunoreactivity is consistently colocalized to neurons and sporadically with astrocytes in the SON. Dual fluorescent colocalization of anti-Thy-1 (a) with anti-oxytocin (b) revealed prominent colocalization of Thy-1-immunoreactivity to oxytocinergic neurons (c, arrows). Still present, but less commonly observed was Thy-1-immunoreactive profiles (d) colocalized to GFAP-immunoreactive astrocytes (e) in the SON (f, arrows). Quantitative analysis of Thy-1-immunoreactivity in the SON was performed using the colocalization colormap script, ImageJ plugin. Analysis demonstrated significantly more Thy-1-immunoreactivity was found in the neurons compared to the astrocytes of the SON (g; $p=0.001$). Each shape on the graph indicates an individual data point with the lines representing the mean and SD. OT, oxytocinergic. Scale bars = 30 μm.
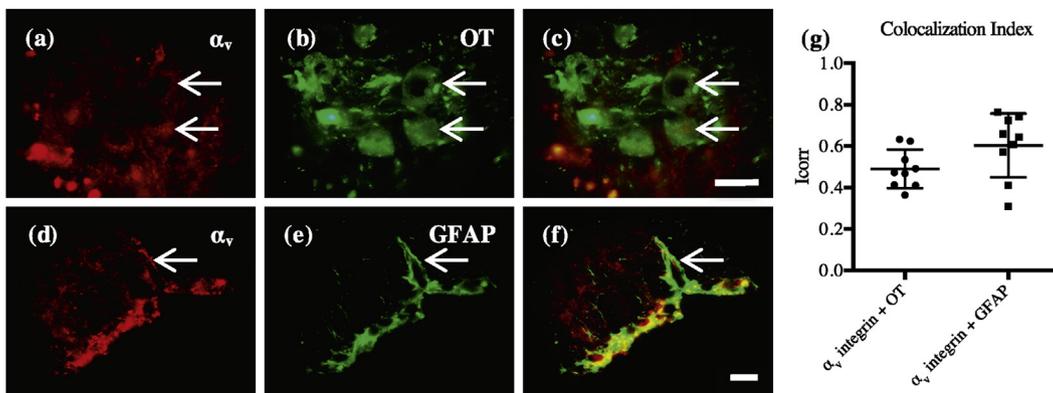
Figure 4. α_V integrin-immunoreactivity is colocalized to neurons and astrocytes in the SON. Dual fluorescent colocalization of anti-α_V integrin (a) with anti-oxytocin (b) revealed α_V integrin-immunoreactivity in oxytocinergic neurons (c, arrows). Strong α_V integrin-immunoreactivity in the VGL of the SON (d) colocalized to GFAP-immunoreactive astrocytes (e) of the SON (f, arrows). Quantitative analysis of α_V integrin-immunoreactivity in the SON was performed using the colocalization colormap script, ImageJ plugin. The results demonstrated similar levels of α_V integrin-immunoreactivity in both neurons and astrocytes of the SON (g; $p=0.0762$). Each shape on the graph indicates an individual data point with the lines representing the mean and SD. OT, oxytocinergic neurons. Scale bars = 30 μm.
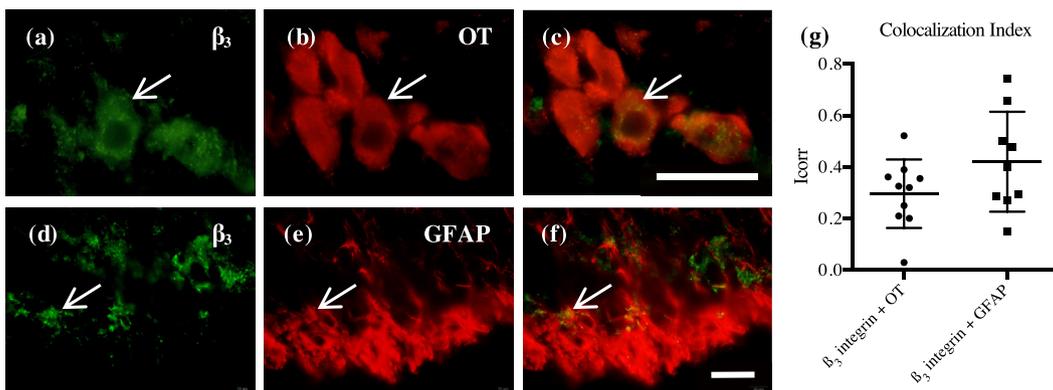
Figure 5. ß$_3$ integrin-immunoreactivity is colocalized to neurons and astrocytes in the SON. Prominent ß$_3$ integrin-immunoreactive profiles (a) were co-localized to oxytocinergic neurons (b) in the SON (c). Consistent ß$_3$ integrin-immunoreactive profiles (d) were also colocalized to GFAP-immunoreactive astrocytes (e) in the VGL of the SON (f). Quantification of ß$_3$ integrin-immunoreactivity in the SON was performed using the colocalization colormap script, ImageJ plugin. Analysis demonstrated consistent levels of ß$_3$ integrin-immunoreactivity in both neurons and astrocytes of the SON (g; $p=0.119$). Each shape on the graph indicates an individual data point with the lines representing the mean and SD. OT, oxytocinergic neuron. Scale bars = 30 μm.
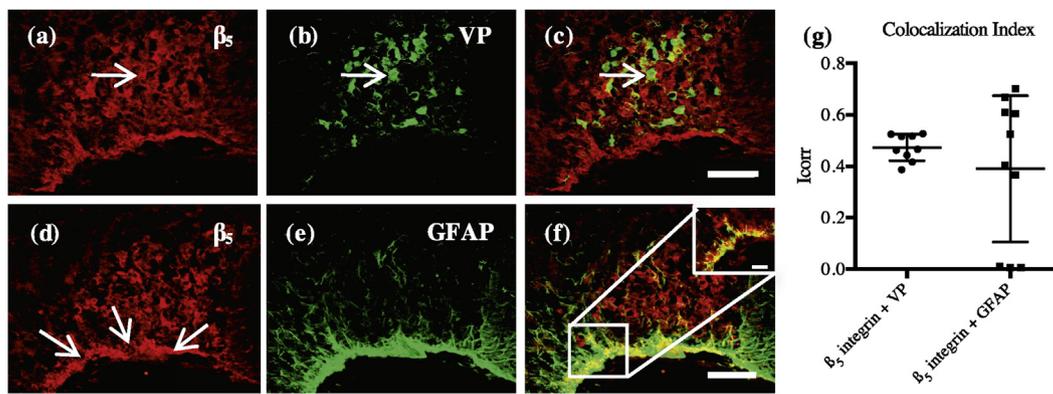
Figure 6. β_5 integrin-immunoreactivity is colocalized to neurons and astrocytes in the SON. Strong β_5 integrin-immunoreactivity was colocalized with vasopressinergic neurons (a–c) and GFAP-immunoreactive astrocytes in the SON (d-f; inset in f). Note the arrows in (d) illustrating β_5 integrin-immunoreactivity highly present in the VGL. Quantification of β_5 integrin-immunoreactivity in the SON was performed using the colocalization colormap script, ImageJ plugin. Analysis demonstrated uniform levels of β_5 integrin-immunoreactivity in both neurons and astrocytes of the SON (g; $p=0.4018$). Each shape on the graph indicates an individual data point with the lines representing the mean and SD. VP, vasopressinergic neuron. Scale bars = 100 µm; Scale bar in inset = 30 µm.

magnocellular neurons in the NL but not to the resident astrocytes of the NL, pituicytes (Miyata et al., 2001). We extended the results of Miyata et al., (2001), and demonstrated Thy-1-immunoreactivity in the somata of the magnocellular neurons in the SON, but unlike the previous report, we found sporadic GFAP-positive astrocytes co-localized with Thy-1-immunoreactivity in the SON. The astrocytes in the SON and the pituicytes in the NL are quite different functionally and in the genes that they express. It should be noted that there are reports demonstrating Thy-1 localization on astrocytes, although these investigators utilized cultured astrocytes (Pruss, 1979; Kennedy et al., 1980; Fields et al., 1982; Hooghe-Peters and Hooghe, 1982; Brown et al., 1984). Nonetheless, it was suggested by Brown et al. (1984), that astrocytic Thy-1 is most abundant on cells in contact with neurons. In the SON, it is well established that the astrocytic processes provide extensive ensheathment of neurons and dendrites by projecting dorsally from the VGL (Salm et al., 1985), providing possible clarification why we observed Thy-1-positive astrocytes in the SON. We also observed α_V integrin-, β_3 integrin-, and β_5 integrin-immunoreactivity on both neurons and astrocytes in the SON, suggesting that astrocytic Thy-1 may be able to bind to neuronal $\alpha_V\beta_3$ or $\alpha_V\beta_5$. However, the results of our integrin colocalization studies do not demonstrate the dimerization of the integrin subunits on the neurons or astrocytes in the SON. Future experiments will be performed to determine what, if any, integrins are dimerized in the SON, what the interacting ligands for Thy-1 are in the SON, and the cells directly involved in these interactions.

In summary, the results presented here demonstrate a significant increase in Thy-1 in the SON of a rat at the age when uninjured axons do not elicit a collateral sprouting response following axotomy. It remains to be determined if the increase in Thy-1 prevents the collateral sprouting response; however, given our recent observations that CNTFRα is significantly decreased in the rat SON at the same age that Thy-1 is elevated, our current hypothesis is that there is not one specific factor that prevents the collateral sprouting response. Rather, we hypothesize that a combination of age-related changes in intrinsic and extrinsic factors occur in the SON that collectively decreases the ability to functionally recover following injury.

Declarations

Author contribution statement

Jason M. Askvig: Conceived and designed the experiments; Contributed reagents, materials, analysis tools or data; Wrote the paper.

Talia S. Dalzell, Nadia Toumeh, Phillip T. Kuball, Sara T. Whiteman, Erik W. Bye, Marissa J. Andersen, Michael G. McCarthy, Riley E. Irmen,

Sydney H. Bexell: Performed the experiments; Analyzed and interpreted the data.

Molly M. Benolken, Brooke L. Maruska, Shelby E. Nordmann: Performed the experiments.

Competing interest statement

The authors declare no conflict of interest.

Additional information

No additional information is available for this paper.

References

Adams, J.H., Daniel, P.M., Prichard, M.M., 1964. Some effects of transection of the pituitary stalk. Br. Med. J. 2, 1619–1625.

Askvig, J.M., Leiphon, L.J., Watt, J.A., 2012. Neuronal activity and axonal sprouting differentially regulate CNTF and CNTF receptor complex in the rat supraoptic nucleus. Exp. Neurol. 233, 243.

Askvig, J.M., Lo, D.Y., Sudbeck, A.W., Behm, K.E., Leiphon, L.J., Watt, J.A., 2013. Inhibition of the Jak-STAT pathway prevents CNTF-mediated survival of axotomized oxytocinergic magnocellular neurons in organotypic cultures of the rat supraoptic nucleus. Exp. Neurol. 240, 75.

Askvig, J.M., Watt, J.A., 2015. The MAPK and PI3K pathways mediate CNTF-induced neuronal survival and process outgrowth in hypothalamic organotypic cultures. J. Cell Commun. Signal. 9, 217.

Askvig, J.M., Watt, J.A., 2019. Absence of axonal sprouting following unilateral lesion in 125-day-old rat supraoptic nucleus may be due to age-dependent decrease in protein levels of ciliary neurotrophic factor receptor alpha. J. Comp. Neurol. 527, 2291–2301.

Avalos, A.M., Arthur, W.T., Schneider, P., Quest, A.F., Burridge, K., Leyton, L., 2004. Aggregation of integrins and RhoA activation are required for Thy-1-induced morphological changes in astrocytes. J. Biol. Chem. 279, 39139–39145.

Avalos, A.M., Labra, C.V., Quest, A.F., Leyton, L., 2002. Signaling triggered by Thy-1 interaction with beta 3 integrin on astrocytes is an essential step towards unraveling neuronal Thy-1 function. Biol. Res. 35, 231–238.

Avalos, A.M., Valdivia, A.D., Munoz, N., Herrera-Molina, R., Tapia, J.C., Lavandero, S., Chiong, M., Burridge, K., Schneider, P., Quest, A.F., Leyton, L., 2009. Neuronal Thy-1 induces astrocyte adhesion by engaging syndecan-4 in a cooperative interaction with alphavbeta3 integrin that activates PKCalpha and RhoA. J. Cell Sci. 122, 3462.

Barlow, J.Z., Huntley, G.W., 2000. Developmentally regulated expression of Thy-1 in structures of the mouse sensory-motor system. J. Comp. Neurol. 421, 215–233.

Brown, R.H., Schweitzer, J., Dichter, M.A., 1984. Expression of the Thy-1 antigen in long-term cultures of embryonic mouse spinal cord. Brain Res. 296, 87–91.

Buga, A.M., Dunoiu, C., Balseanu, A., Popa-Wagner, A., 2008a. Cellular and molecular mechanisms underlying neurorehabilitation after stroke in aged subjects. Rom. J. Morphol. Embryol. 49, 279.

Buga, A.M., Sascau, M., Pisoschi, C., Herndon, J.G., Kessler, C., Popa-Wagner, A., 2008b. The genomic response of the ipsilateral and contralateral cortex to stroke in aged rats. J. Cell Mol. Med. 12, 2731.

Deacon, R.M., Rawlins, J.N., 1996. Equithesin without chloral hydrate as an anaesthetic for rats. Psychopharmacology 124, 288–290.

Doherty, P., Singh, A., Rimon, G., Bolsover, S.R., Walsh, F.S., 1993. Thy-1 antibody-triggered neurite outgrowth requires an influx of calcium into neurons via N- and L-type calcium channels. J. Cell Biol. 122, 181.

Dreyer, E.B., Leifer, D., Heng, J.E., McConnell, J.E., Gorla, M., Levin, L.A., Barnstable, C.J., Lipton, S.A., 1995. An astrocytic binding site for neuronal Thy-1 and its effect on neurite outgrowth. Proc. Natl. Acad. Sci. U. S A 92, 11195.

Fields, K.L., Currie, D.N., Dutton, G.R., 1982. Development of Thy-1 antigen on cerebellar neurons in culture. J. Neurosci. 2, 663–673.

Gardiner, N.J., Fernyhough, P., Tomlinson, D.R., Mayer, U., von der Mark, H., Streuli, C.H., 2005. Alpha7 integrin mediates neurite outgrowth of distinct populations of adult sensory neurons. Mol. Cell. Neurosci. 28, 229.

Gardiner, N.J., Moffatt, S., Fernyhough, P., Humphries, M.J., Streuli, C.H., Tomlinson, D.R., 2007. Preconditioning injury-induced neurite outgrowth of adult rat sensory neurons on fibronectin is mediated by mobilisation of axonal alpha5 integrin. Mol. Cell. Neurosci. 35, 249.

Georges-Labouesse, E., Mark, M., Messaddeq, N., Gansmuller, A., 1998. Essential role of alpha 6 integrins in cortical and retinal lamination. Curr. Biol. 8, 983.

Gupton, S.L., Gertler, F.B., 2010. Integrin signaling switches the cytoskeletal and exocytic machinery that drives neuritogenesis. Dev. Cell 18, 725.

Harper, M.M., Ye, E.A., Blong, C.C., Jacobson, M.L., Sakaguchi, D.S., 2010. Integrins contribute to initial morphological development and process outgrowth in rat adult hippocampal progenitor cells. J. Mol. Neurosci. 40, 269.

Hermosilla, T., Munoz, D., Herrera-Molina, R., Valdivia, A., Munoz, N., Nham, S.U., Schneider, P., Burridge, K., Quest, A.F., Leyton, L., 2008. Direct Thy-1/alphaVbeta3 integrin interaction mediates neuron to astrocyte communication. Biochim. Biophys. Acta 1783, 1111.

Herrera-Molina, R., Frischknecht, R., Maldonado, H., Seidenbecher, C.I., Gundelfinger, E.D., Hetz, C., Aylwin Mde, L., Schneider, P., Quest, A.F., Leyton, L., 2012. Astrocytic alphaVbeta3 integrin inhibits neurite outgrowth and promotes retraction of neuronal processes by clustering Thy-1. PloS One 7, e34295.

Herrera-Molina, R., Valdivia, A., Kong, M., Alvarez, A., Cardenas, A., Quest, A.F., Leyton, L., 2013. Thy-1-interacting molecules and cellular signaling in cis and trans. Int. Rev. Cell Mol. Biol. 305, 163.

Hooghe-Peters, E.L., Hooghe, R.J., 1982. The Thy-1 glycoprotein on nerve cells in culture: electron-microscopic analysis and biochemical characterization. J. Neuroimmunol. 2, 191–200.

Jaerve, A., Schiwy, N., Schmitz, C., Mueller, H.W., 2011. Differential effect of aging on axon sprouting and regenerative growth in spinal cord injury. Exp. Neurol. 231, 284.

Jaskolski, F., Mulle, C., Manzoni, O.J., 2005. An automated method to quantify and visualize colocalized fluorescent signals. J. Neurosci. Methods 146, 42–49.

Kang, S.S., Keasey, M.P., Cai, J., Hagg, T., 2012. Loss of neuron-astroglial interaction rapidly induces protective CNTF expression after stroke in mice. J. Neurosci. 32, 9277–9287.

Kawamoto, K., Kawashima, S., 1985. Plasticity of vasopressin- and oxytocin-containing fibers in the median eminence in hypophysectomized young and old mice. Brain Res. 330, 189.

Keasey, M.P., Kang, S.S., Lovins, C., Hagg, T., 2013. Inhibition of a novel specific neuroglial integrin signaling pathway increases STAT3-mediated CNTF expression. Cell Commun. Signal. 11, 35.

Kennedy, P.G., Lisak, R.P., Raff, M.C., 1980. Cell type-specific markers for human glial and neuronal cells in culture. Lab. Invest. 43, 342–351.

Kiernan, J.A., 1970. Two types of axonal regeneration in the neurohypophysis of the rat. J. Anat. 107, 187.

Kiernan, J.A., 1971. Pituicytes and the regenerative properties of neurosecretory and other axons in the rat. J. Anat. 109, 97.

Leyton, L., Schneider, P., Labra, C.V., Ruegg, C., Hetz, C.A., Quest, A.F., Bron, C., 2001. Thy-1 binds to integrin beta(3) on astrocytes and triggers formation of focal contact sites. Curr. Biol. 11, 1028.

Luo, J.M., Geng, Y.Q., Zhi, Y., Zhang, M.Z., van Rooijen, N., Cui, Q., 2010. Increased intrinsic neuronal vulnerability and decreased beneficial reaction of macrophages on axonal regeneration in aged rats. Neurobiol. Aging 31, 1003.

McLean, I.W., Nakane, P.K., 1974. Periodate-lysine-paraformaldehyde fixative. A new fixation for immunoelectron microscopy. J. Histochem. Cytochem. 22, 1077.

Miyata, S., Takamatsu, H., Maekawa, S., Matsumoto, N., Watanabe, K., Kiyohara, T., Hatton, G.I., 2001. Plasticity of neurohypophysial terminals with increased hormonal release during dehydration: ultrastructural and biochemical analyses. J. Comp. Neurol. 434, 413.

Moll, J., 1957. Regeneration of the supraoptico-hypophyseal and paraventriculo-hypophyseal tracts in the hypophysectomized rat. Z. Zellforsch. Mikrosk. Anat. 46, 686.

Moll, J., de Wied, 1962. Observations on the hypothalamoposthypophyseal system of the posterior lobectomized rat. Gen. Comp. Endocrinol. 2, 215–228.

Morris, R., Grosveld, F., 1989. Expression of Thy-1 in the nervous system of the rat and mouse. Immunol. 45, 121.

Polenov, A.L., Ugrumov, M.V., Propp, M.V., Belenky, M.A., 1974. The hypothalamo-hypophysial system of hypophysectomized rats. I. Ultrastructure of nerve fibres in "intact" and dehydrated animals. Cell Tissue Res. 155, 541–554.

Pruss, R.M., 1979. Thy-1 antigen on astrocytes in long-term cultures of rat central nervous system. Nature 280, 688–690.

Raisman, G., 1973. Electron microscopic studies of the development of new neurohaemal contacts in the median eminence of the rat after hypophysectomy. Brain Res. 55, 245.

Rusnak, M., House, S.B., Arima, H., Gainer, H., 2002. Ciliary neurotrophic factor increases the survival of magnocellular vasopressin and oxytocin neurons in rat supraoptic nucleus in organotypic cultures. Microsc. Res. Tech. 56, 101.

Rusnak, M., House, S.B., Gainer, H., 2003. Long-term effects of ciliary neurotrophic factor on the survival of vasopressin magnocellular neurones in the rat supraoptic nucleus in vitro. J. Neuroendocrinol. 15, 933.

Salm, A.K., Smithson, K.G., Hatton, G.I., 1985. Lactation-associated redistribution of the glial fibrillary acidic protein within the supraoptic nucleus. An immunocytochemical study. Cell Tissue Res. 242, 9.

Shapiro, L., Love, J., Colman, D.R., 2007. Adhesion molecules in the nervous system: structural insights into function and diversity. Annu. Rev. Neurosci. 30, 451.

Shetty, A.K., Turner, D.A., 1998. Hippocampal interneurons expressing glutamic acid decarboxylase and calcium-binding proteins decrease with aging in Fischer 344 rats. J. Comp. Neurol. 394, 252.

Tiveron, M.C., Barboni, E., Pliego Rivero, F.B., Gormley, A.M., Seeley, P.J., Grosveld, F., Morris, R., 1992. Selective inhibition of neurite outgrowth on mature astrocytes by Thy-1 glycoprotein. Nature 355, 745.

Vogelezang, M., Forster, U.B., Han, J., Ginsberg, M.H., French-Constant, C., 2007. Neurite outgrowth on a fibronectin isoform expressed during peripheral nerve regeneration is mediated by the interaction of paxillin with alpha4beta1 integrins. BMC Neurosci. 8, 44.

Vutskits, L., Bartanusz, V., Schulz, M.F., Kiss, J.Z., 1998. Magnocellular vasopressinergic neurons in explant cultures are rescued from cell death by ciliary neurotrophic factor and leukemia inhibiting factor. Neuroscience 87, 571.

Watt, J.A., Bone, S., Pressler, M., Cranston, H.J., Paden, C.M., 2006. Ciliary neurotrophic factor is expressed in the magnocellular neurosecretory system of the rat in vivo: evidence for injury- and activity-induced upregulation. Exp. Neurol. 197, 206.

Watt, J.A., Lo, D., Cranston, H.J., Paden, C.M., 2009. CNTF receptor alpha is expressed by magnocellular neurons and expression is upregulated in the rat supraoptic nucleus during axonal sprouting. Exp. Neurol. 215, 135.

Watt, J.A., Moffet, C.W., Zhou, X., Short, S., Herman, J.P., Paden, C.M., 1999. Central peptidergic neurons are hyperactive during collateral sprouting and inhibition of activity suppresses sprouting. J. Neurosci. 19, 1586.

Watt, J.A., Paden, C.M., 1991. Compensatory sprouting of uninjured magnocellular neurosecretory axons in the rat neural lobe following unilateral hypothalamic lesion. Exp. Neurol. 111, 9.

Xue, G.P., Calvert, R.A., Morris, R.J., 1990. Expression of the neuronal surface glycoprotein Thy-1 is under post-transcriptional control, and is spatially regulated, in the developing olfactory system. Development 109, 851–864.

Xue, G.P., Rivero, B.P., Morris, R.J., 1991. The surface glycoprotein Thy-1 is excluded from growing axons during development: a study of the expression of Thy-1 during axogenesis in hippocampus and hindbrain. Development 112, 161–176.

Zhou, Y., Hagood, J.S., Lu, B., Merryman, W.D., Murphy-Ullrich, J.E., 2010. Thy-1-integrin alphav beta5 interactions inhibit lung fibroblast contraction-induced latent transforming growth factor-beta1 activation and myofibroblast differentiation. J. Biol. Chem. 285, 22382.